Physiological Concentrations of Divalent Magnesium Ion Activate the Serine/Threonine Specific Protein Kinase ERK2†

William F. Waas‡ and Kevin N. Dalby*,‡,§

Division of Medicinal Chemistry, College of Pharmacy, and Graduate Programs in Biochemistry and Molecular Biology and Center for Molecular and Cellular Toxicology, University of Texas at Austin, Austin, Texas 78712

Received November 13, 2002; Revised Manuscript Received January 9, 2003

ABSTRACT: Extracellular regulated protein kinase 2 (ERK2) is a eukaryotic protein kinase whose activity is regulated by phorbol esters, serum, and growth factors, and displays enhanced activity in several human tumors. Despite its important biological function, its mechanism of catalysis and mode of regulation are poorly understood. Recently, we showed that in the presence of 10 mM magnesium chloride, ERK2 phosphorylates the transcription factor Ets-1 through a random-ordered ternary-complex mechanism [Waas, W. F., and Dalby, K. N. (2002) *J. Biol. Chem. 277*, 12532]. Now we provide kinetic evidence that ERK2 must bind two divalent magnesium ions to facilitate catalysis at a physiologically relevant rate, because a second magnesium ion promotes both $MgATP^{2-}$ binding and phosphoryl transfer. The velocity dependence on magnesium at saturating concentrations of the protein substrate, EtsΔ138, over a range of ATP^{4-} and Mg^{2+} ion concentrations, supports the notion that magnesium is an *essential* activator of ERK2. At high (≥1 mM) concentrations of ATP^{4-}, the velocity dependence on total Mg^{2+} is sigmoidal, but plateaus at high concentrations of free Mg^{2+}, where the enzyme is fully activated. At concentrations of Mg^{2+} of ≤4 mM, the velocity dependence on ATP^{4-} displays a peak when the concentration of ATP^{4-} approaches that of total Mg^{2+} and tends to zero at high concentrations of ATP^{4-}, where the enzyme is predominantly unactivated. The observed velocity dependencies are consistent with the notion that ERK2·EtsΔ138 complexes and ATP^{4-} compete for the same pool of Mg^{2+} ions in solution. No binding of ATP^{4-} (0−2.5 mM) by ERK2 (65 μM) can be detected using isothermal titration calorimetry at 27 °C, pH 8.0, and an ionic strength of 0.15 M (KCl), suggesting that the complex, $MgATP^{2-}$, is the true substrate for ERK2. In contrast, 5-iodotubericidin binds ERK2 tightly (K_d = 1 μM) and displays a competitive inhibition pattern toward $MgATP^{2-}$ and a mixed pattern toward free Mg^{2+}, suggesting that the binding of Mg^{2+} before $MgATP^{2-}$ is not compulsory.

Protein kinases catalyze the phosphorylation of proteins to form phosphate monoesters of serine, threonine, or tyrosine (*1*). These modifications can have a dramatic impact on protein function and consequently underlie many aspects of signal transduction. The phosphate donor is usually the magnesium complex of adenosine triphosphate, although the protein kinase CK2 is known to utilize the guanosine triphosphate complex (*2*−*4*). Until recently, all protein kinases were thought to be structurally related, harboring a highly conserved catalytic domain of some 300 amino acids that adopts a conserved protein fold, focused around several key catalytic residues. However, several novel protein kinases have been identified recently, suggesting that the protein kinase family is likely to be more diverse in structure and sequence than originally thought (*5*−*8*).

While the conserved nature of the protein kinase catalytic core implies a conserved chemical mechanism, protein kinase regulation is extremely varied in nature (*9*). We have been interested in the mechanism and regulation of the extracellular regulated protein kinases, ERK1 and ERK2,[1] for some time, because of their key roles in cellular signal transduction. They phosphorylate a large number of structurally disparate proteins upon activation by phorbol esters, serum, and growth factors and are activated through a protein kinase cascade, termed the mitogen-activated protein kinase (MAPK) pathway, usually by Ras, a small guanine nucleotide binding protein that transduces extracellular signals to the cell nucleus (*10*). This pathway has received considerable attention in recent years, because the expression of several proto-oncogenes, including *ras* itself, can lead to the activation of ERK1 and ERK2 in a constitutive manner, which is causatively linked to the transformed phenotype in many cells types (*11*). MAPKK, a dual specific protein kinase, whose inhibition can revert this phenotype, mediates the activation of ERK1 and ERK2 directly. Recent studies in colon

† This research was supported in part by the Welch Foundation (Grant F-1390), the National Institutes of Health (Grant GM59802), and Analytical Instrumentation Facility Core Grant P30 ES07784. W.F.W. was a recipient of a National Research Service Award, NIH Biotechnology Predoctoral Training Grant T32 GM08474.

* To whom correspondence should be addressed: Division of Medicinal Chemistry, College of Pharmacy, University of Texas at Austin, Austin, TX 78712. Telephone: (512) 471-9267. Fax: (512) 232-2606. E-mail: Dalby@mail.utexas.edu.

‡ Division of Medicinal Chemistry, College of Pharmacy.

§ Graduate Programs in Biochemistry and Molecular Biology and Center for Molecular and Cellular Toxicology.

[1] Abbreviations: ERK2, extracellular regulated protein kinase 2; EtsΔ138, polyhistidine-tagged Ets-1(1−138); EtsΔ138∼P, polyhistidine-tagged Ets-1(1−138) phosphorylated at Thr-38; cAPK, cyclic AMP-dependent protein kinase; MAPK, mitogen-activated protein kinase; MAPKK, mitogen-activated protein kinase kinase; A_{280}, absorbance at 280 nm; PP_i, pyrophosphate; 5-IT, 5-iodotubericidin.

10.1021/bi027171w CCC: $25.00
Published on Web 02/22/2003

Scheme 1: Phosphorylation of EtsΔ138 by ERK2[a]

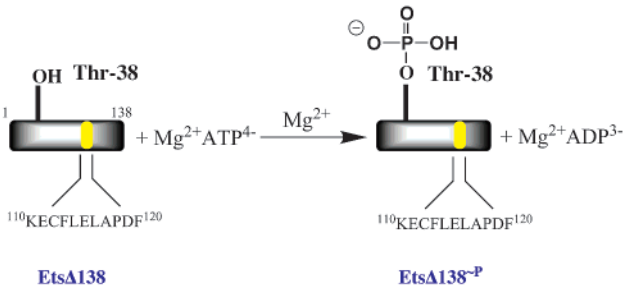

[a] ERK2 catalyzes the phosphorylation of EtsΔ138 on Thr-38. Amino acids 110−120 represent a putative ERK2 docking site thought to facilitate the reaction (*17*).

carcinomas showed that a highly specific and potent inhibitor of MAPKK, PD 184352, elicits a promising level of antitumor efficacy *in vivo* (*12*). Therefore, specific inhibitors for ERK1 and ERK2, which are the only known substrates of MAPKK, are likely to be extremely useful.

While the screening of large libraries of compounds to identify enzyme inhibitors is a powerful method employed in the pharmaceutical industry, an alternative approach based on chemical and mechanistic knowledge, often called rational drug design, can open up new avenues of mechanistic inquiry and potentially new classes of inhibitors. Taking this approach requires an understanding of the catalytic mechanism of an enzyme. As our mechanistic knowledge of ERK1 and ERK2 is limited, one current focus in our laboratory is the delineation of their catalytic mechanisms. ERK2 catalyzes the transfer of the γ-phosphate of adenosine triphosphate to serine or threonine residues found as Ser-Pro or Thr-Pro motifs on proteins. While the proline is believed to be critical, further specificity is conferred through protein−substrate docking domains, where at least one specific interaction is made between ERK2 and the protein on a locus that lies outside of the active site (*13*). To study these enzymes, we developed a globular protein substrate for ERK2 termed EtsΔ138 (*14*, *15*) comprising residues 1−138 of transcription factor Ets-1, which is believed to be a substrate of ERK2 *in vivo* and which contains an ERK2 docking site (Scheme 1) (*16*, *17*).

Protein kinases catalyze a thermodynamically favorable reaction where the hydroxyl nucleophile of a serine, threonine, or tyrosine displaces the good ADP^{3-} leaving group (pK_a of $ADPH^{2-} = 6.5$) from the γ-phosphate of ATP. While the phosphoryl donor for most kinases is generally thought to be the magnesium complex of the tetra-anion of adenosine triphosphate (ATP^{4-}), an additional magnesium ion is implicated in the mechanism of a number of protein kinases. By far the most extensively characterized protein kinase is cAMP-dependent protein kinase (cAPK), an important protein kinase that is activated in response to the second messenger cAMP. A number of years ago, electron paramagnetic resonance studies by Armstrong et al. (*18*) demonstrated that with ATP^{4-} bound there are two divalent metal ion binding sites within the active site of cAPK, one of high affinity and one of low affinity. Subsequently, Zheng et al. reported the crystal structure of the catalytic subunit of cAMP-dependent protein kinase complexed with $MgATP^{2-}$ and a peptide inhibitor. This work and studies, with Mg^{2+} replaced with Mn^{2+}, provided the first *crystallographic*

Scheme 2: Metal Ion Coordination of (A) cAPK and (B) the Insulin Receptor

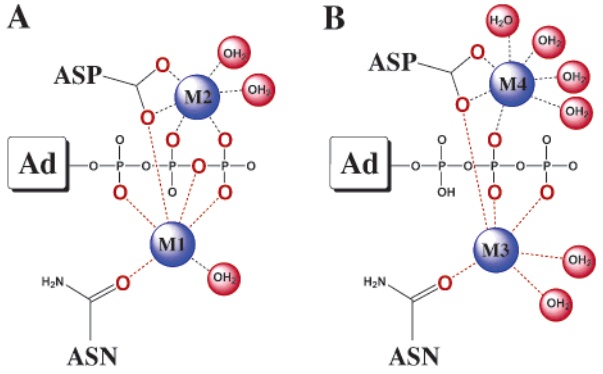

information about the coordination of these two Mg^{2+} ions. These structures showed that a Mg^{2+} ion, bound at the higher-affinity M2 site (depicted in Scheme 2A), is octahedrally coordinated to six oxygen atoms comprising the β- and γ-phosphates of ATP^{4-}, two atoms from Asp-165, and two water molecules. The low-affinity magnesium ion (M1 site in Scheme 2A) is octahedrally coordinated by the α- and γ-phosphates of ATP^{4-}, the bridging oxygen, one oxygen atom of Asp-165, the side chain carbonyl of Asn-171, and one water molecule (*19*). In recent years, the structures of several other protein serine/threonine kinases bound to ATP^{4-} have been reported (*3*, *20*, *21*). The magnesium coordination within all these structures is conserved. Of particular relevance to ERK2 is the structure of the unactivated (not phosphorylated) form of MAPK JNK3, complexed to the ATP analogue AMPPNP (*21*). Its coordination of two Mg^{2+} ions is indistinguishable from that of cAPK (Scheme 2A) and provided the basis for the prediction that ERK2 utilizes Mg^{2+} in a manner analogous to that of cAPK.

Despite extensive structural information, the precise functions of the two divalent magnesium ions in cAPK are not fully resolved. A pre-steady state kinetic study suggested that the high-affinity M2 Mg^{2+} ion is both necessary and sufficient for the fast accumulation of a phosphorylated peptide on cAPK. Surprisingly, the low-affinity M1 Mg^{2+} ion is not essential for phosphoryl transfer (*22*, *23*). It is not immediately clear why this is the case, because in the structure of cAPK complexed with a transition state mimic, both the M1 and M2 magnesium ions are intimately associated with moieties undergoing covalency changes (*24*). Interestingly, the occupancy of the low-affinity site appears to increase the affinity of cAPK for $MgATP^{2-}$ (*25*) and $MgADP^{-}$ (*18*), while also inhibiting the rate-limiting product release step (*23*).

In a previous study, we examined the substrate and product dependence of ERK2 and concluded that ERK2 follows a random-ordered ternary-complex mechanism (*15*). However, because in this study the concentration of magnesium was at a saturating level, the kinetic analysis was essentially transparent to its role. Therefore, given the likelihood that ERK2 coordinates two Mg^{2+} ions in a manner analogous to that of JNK3, we decided to examine the sensitivity of ERK2 to divalent magnesium ions. We report the surprising result that, in contrast to cAPK, ERK2 must bind two divalent magnesium ions to facilitate phosphoryl transfer at a physiologically relevant rate. In this process, a second magnesium ion appears to be an essential activator of ERK2.[2]

EXPERIMENTAL PROCEDURES

Buffers, Proteins, and Reagents. Trizma base was from EM Industries (Gibbstown, NJ). Sigma (St. Louis, MO) provided all other buffer components and chemicals. Qiagen Inc. (Santa Clarita, CA) supplied Ni−NTA agarose. Kinase assays were conducted with Roche (Indianapolis, IN) special quality sodium adenosine triphosphate ($Na_2^+ATPH_2^{2-}$) and [γ-^{32}P]$(NH_4^+)_4ATP^{4-}$ from ICN (Costa Mesa, CA). Plasmids used to express (His_6-tagged) ERK2 (*26*) and (His_6-tagged) Ets1(1−138) (*27*) have been reported previously. Stock solutions of $Na_2^+ATPH_2^{2-}$ were titrated to pH 8.0 with potassium hydroxide. All concentrations were determined spectrophotometrically at 259 nm, assuming an extinction coefficient ϵ of 15 400 cm^{-1} M^{-1}. The amount of hydrolyzable ATP^{4-} was determined using a hexokinase−glucose-6-phosphate dehydrogenase coupled assay. Spectral changes during coupled assays (NADH−NAD^+) were monitored at 340 nM using an extinction coefficient ϵ of 6300 cm^{-1} M^{-1} to calculate adenosine triphosphate concentrations. Comparison of the two methods gave values that differed by less than 2%. The expression of hexahistidine-tagged ERK2 and EtsΔ138 in *Escherichia coli* has been described previously (*15*). According to the method of Gill and von Hippel (*28*), absorbance measurements at 280 nm were used to determine protein concentrations after calibration by amino acid analysis.

Kinetic Measurements. Protein kinase assays were conducted at 27 °C and pH 8.0 maintained with 25 mM HEPES, containing 2 nM ERK2, 5−150 μM EtsΔ138, 0.02−4.3 mM [γ-^{32}P]ATP^{4-} (100−1000 cpm/pmol), and 0.5 μg/mL BSA (bovine serum albumin) in a final volume of 50−100 μL. The ionic strength was maintained at 0.15 M with KCl.[3] At low concentrations of total magnesium (Mg_0^{2+}), the formation of K^+ATP^{4-} is significant, because variable concentrations of KCl were included in the kinetic assay to keep the ionic strength constant. Therefore, the concentration of kinetically significant ionic species was determined using empirically determined dissociation constants for $Mg^{2+}ATP^{4-}$ and K^+ATP^{3-} (see below). Several control experiments served to show that while potassium ions can influence the enzyme velocity these effects are minor and essentially within experimental error. For example, at 2 mM Mg^{2+} and excess ATP^{4-} (4 mM), the observed velocity varied from 0.86 to 1.25 s^{-1} when the K^+ concentration was varied from 40 to 100 mM. This is attributed to activation of ERK2 by the displacement of Mg^{2+} from the pool of $MgATP^{2-}$ in solution. At equimolar Mg^{2+} and ATP^{4-} concentrations (4 mM), the observed velocity decreases by 12% when the K^+ concentration is varied from 40 to 100 mM, whereas at 10 mM Mg^{2+}, the change is even smaller (5%).

The dependence of the reaction on substrate concentration was assessed by measurement of initial rates, under conditions where total product formation represented less than 10% of the initial substrate concentrations. The reaction mixture was incubated for 5 min before the reaction was initiated by the addition of the enzyme. Aliquots (5−10 μL) were taken at set time points and applied to 2 cm × 2 cm P81 cellulose paper. The papers were washed for 3 × 10 min in 50 mM phosphoric acid (H_3PO_4) and then in acetone and dried, and the amount of labeled protein was determined by counting the associated counts per minute on a Packard 1500 scintillation counter at 2σ in the presence of scintillant.

Scheme 3

$$K^+ATP^{4-} + Mg^{2+} \underset{}{\overset{K'_0}{\rightleftharpoons}} ATP^{4-} + K^+ + Mg^{2+} \underset{K_0}{\rightleftharpoons} Mg^{2+}ATP^{4-} + K^+$$

Determining the Concentrations of Free and Complexed Anions and Cations. The calculation of the concentrations of the species shown in Scheme 3 by numerical integration of eqs 1−5 using the program Scientist (Micromath) required measurement of the two experimentally determined dissociation constants (K_0' and K_0) and the concentrations of total ATP^{4-} (ATP_0^{4-}), total magnesium (Mg_0^{2+}), and total potassium (K_0^+) under the conditions of the kinetic assay. K_0 and K_0' were determined by fluorescence measurements performed under the standard conditions of the kinetic assays in a 1 mL quartz cuvette following published methods using the fluorescent indicator 8-hydroxyquinoline (*29*−*31*). The values that were obtained (K_0 = 31 μM and K_0' = 66 mM) are in good agreement with published values (*29*).

$$K_0 = ([Mg_F^{2+}][ATP_F^{4-}])/[Mg^{2+}ATP^{4-}] \quad (1)$$

$$K_0' = ([K_F^+][ATP_F^{4-}])/[K^+ATP^{4-}] \quad (2)$$

$$[Mg_0^{2+}] = [Mg_F^{2+}] + [Mg^{2+}ATP^{4-}] \quad (3)$$

$$[ATP_0^{4-}] = [ATP_F^{4-}] + [K^+ATP^{4-}] + [Mg^{2+}ATP^{4-}] \quad (4)$$

$$[K_0^+] = [K_F^+] + [K^+ATP^{4-}] \quad (5)$$

Data Analysis.[4] Initial rates (v) were determined by linear least-squares fitting to plots of product versus time. Reciprocal plots of $1/v$ versus $1/s$ were checked for linearity using eq 6, before the data were fitted to eq 7 using a nonlinear least-squares approach, assuming equal variance for velocities, using the program Kaleidagraph 3.5 (Synergy Software).

$$\frac{v}{[E_0]} = \frac{k_{cat}^{app} s}{K_{mS}^{app} + s} \quad (6)$$

$$\frac{v}{[E_0]} = \frac{k_{cat} ab}{K_{iA}K_{mB} + K_{mA}b + K_{mB}a + ab} \quad (7)$$

[2] The term "essential" is used to indicate that activation by a second magnesium ion leads to an *at least* 10-fold increase in the catalytic constant for ERK2.

[3] The ionic strength varied slightly from 0.13 to 0.15 M through slight variations in the composition of ions.

[4] The parameters used in deriving the equations are defined as follows: v, observed velocity; k_{cat}, catalytic constant; k_{cat}^{app}, apparent catalytic constant; K_{mS}^{app}, apparent Michaelis constant for substrate S; a, b, and s, concentrations of A, B, and S, respectively; i, concentration of inhibitor I; K_{iA}, inhibition constant for substrate A; K_{iB}, inhibition constant for substrate B; K_{mA}, Michaelis constant for substrate A; K_{mB}, Michaelis constant for substrate B; K_{iC}^{app}, apparent specific inhibition constant for inhibitor I; K_{iU}^{app}, apparent uncompetitive inhibition constant for inhibitor I; $[ATP_0^{4-}]$, $[Mg_0^{2+}]$, and $[K_0^+]$, total ATP^{4-}, Mg^{2+}, and K^+ concentrations, respectively; $[ATP_F^{4-}]$ and $[Mg_F^{2+}]$, free ATP^{4-} and Mg^{2+} ion concentrations, respectively; K_0' and K_0, dissociation constants for K^+ATP^{4-} and $Mg^{2+}ATP^{4-}$, respectively.

The intercepts $1/k_{cat}^{app}$ and slopes $K_{mS}^{app}/k_{cat}^{app}$ obtained from these fits were then plotted versus either the inhibitor concentration (i) (for inhibition experiments) or the reciprocal of the nonvaried substrate concentration ($1/s$) (for initial velocity experiments). These secondary plots were used to determine the appearance of the overall kinetic equation (*32*). Values for kinetic constants were then obtained using the program Scientist (Micromath) by fitting the kinetic data to the relevant overall equation by global fitting. Data conforming to a sequential initial velocity pattern were fitted to eq 7; data conforming to linear competitive inhibition were fitted to eq 8, and data conforming to linear mixed inhibition were fitted to eq 9. The apparent Michaelis−Menten parameters were determined using eqs 10 and 11 (*32*).

$$\frac{v}{[E_0]} = \frac{k_{cat}^{app} s}{K_{mS}^{app}(1 + i/K_{iC}^{app}) + s} \quad (8)$$

$$\frac{v}{[E_0]} = \frac{k_{cat}^{app} s}{K_{mS}^{app}(1 + i/K_{iC}^{app}) + (1 + i/K_{iU}^{app})s} \quad (9)$$

$$k_{cat}^{app} = \frac{k_{cat} b}{K_{mB} + b} \quad (10)$$

$$K_{mA}^{app} = \frac{K_{iA}K_{mB} + K_{mA}b}{K_{mB} + b} \quad (11)$$

$$\frac{v}{[E_0]} = \frac{k_{cat}[Mg_F^{2+}][Mg^{2+}ATP^{4-}]}{K_{iA}K_{mB} + K_{mA}[Mg_F^{2+}] + K_{mB}[Mg^{2+}ATP^{4-}] + [Mg^{2+}ATP^{4-}][Mg_F^{2+}]} \quad (12)$$

$$\frac{v}{[E_0]} = \frac{k_{cat}[Mg_F^{2+}][MgATP^{2-}] + k_{cat}'K_{mA}[MgATP^{2-}]}{K_{iA}K_{mB} + K_{mA}[Mg_F^{2+}] + K_{mB}[MgATP^{2-}] + [MgATP^{2-}][Mg_F^{2+}]} \quad (13)$$

Initial rates (v) were also obtained over an extensive range of Mg_0^{2+} and ATP_0^{4-} concentrations. These rates were fitted to various kinetic models by global fitting analysis, where individual parameters were first estimated from experiments where the observed data exhibit a strong dependence on them. These parameters were then introduced into a model and allowed to float over a small range (±30%). Refinement of the model corresponded to a good global minimum, the sum of squares, the residual, and the skewness of the indicated values.

Isothermal Calorimetry. Titrations were conducted on a MCS titration calorimeter (MicroCal Inc.) at 27 °C in 25 mM HEPES (pH 8.0), 100 mM KCl, and 0.1% BME (v/v). The same buffer was also used as a reference solution. ERK2 (12.5−60 μM) was titrated with concentrated ligand stocks (125 μM 5-iodotubercidin or 20 mM ATP^{4-} that was in the same buffer). Titrations were initiated with one 2 μL injection of ligand followed by twenty-three 10 μL injections. Blank runs were done in the absence of ERK2. The thermogram was integrated, and blanks were subtracted. Origin 2.3 data analysis software (MicroCal Inc.) was used for integration and fitting to a simple one-binding site model. Data fitting produces values for the binding stoichiometry (n), dissociation constant (K_d), and molar enthalpy change (ΔH). The change in molar entropy (ΔS) and the Gibbs free energy (ΔG) were calculated from the appropriate thermodynamic relationships.

Table 1: Apparent Steady State Michaelis−Menten Parameters for the Phosphorylation of EtsΔ138 by ERK2 at Varied Concentrations of Free Magnesium[a]

$[Mg_F^{2+}]$[b] (mM)	K_{mA}^{app} [c] (μM)	K_{mC}^{app} [c] (μM)	k_{cat}^{app} [c] (s^{-1})
1.0	715 ± 43	10.2 ± 0.4	12.7 ± 0.3
2.0	438 ± 21	13.3 ± 1	18.0 ± 0.3
3.0	342 ± 13	nd	19.0 ± 0.3
10.0	238 ± 21	20.7 ± 0.4	20.2 ± 0.53
20.0	134 ± 8	nd	21.2 ± 0.3

[a] Initial velocities were measured using 2 nM ERK2 and 2 mM DTT at pH 8.0, 27 °C, and an ionic strength of 0.15 M (KCl). [b] Calculated from $[Mg_0^{2+}]$, $[K_0^+]$, and $[ATP_0^{4-}]$ according to eqs 1−5. [c] Determined by plotting v vs s and solving for k_{cat}^{app}, K_{mA}^{app}, and K_{mC}^{app} according to eq 6.

RESULTS AND DISCUSSION

Evidence that ERK2 Binds Two Magnesium Ions. To examine the possibility that the protein serine/threonine kinase ERK2 binds two Mg^{2+} ions, the reaction in Scheme 1 was examined. In the initial experiments described here, the concentration of magnesium was maintained in sufficient excess of ATP^{4-} to avoid possible complications due to the dissociation of the $MgATP^{2-}$ complex. The dependence of product formation (EtsΔ138∼P) on the concentrations of the two substrates, $MgATP^{2-}$ and EtsΔ138, at different fixed concentrations of free magnesium, Mg_F^{2+}, was determined by the method of initial rates. Under these conditions, the appearance of EtsΔ138∼P was linear with time and the kinetic parameters that were obtained were reproducible to within 10%.

The apparent Michaelis constants, K_{mC}^{app}, for EtsΔ138 were measured at Mg_F^{2+} concentrations of 1, 2, and 10 mM. They appear to increase from approximately 10 to 20 μM over this range (Table 1); however, the data are insufficient for defining a correlation. In contrast, the apparent Michaelis constant, K_{mA}^{app}, for $MgATP^{2-}$ clearly decreases, as the concentration of Mg_F^{2+} is increased, by approximately 4.6-fold from 670 to 146 μM (Figure 1A) over the slightly wider Mg_F^{2+} concentration range of 1−20 mM (Table 1). As the tetravalent ATP^{4-} ion is fully complexed to Mg^{2+} under these conditions, we attribute the observed changes in K_{mA}^{app} (and probably K_{mC}^{app}) to the binding of an additional Mg^{2+} ion. A similar conclusion was reached by others studying related protein kinases (*25*, *33*). In the case of cAPK, the affinity of binding of two Mg^{2+} ions to its active site correlates with its kinetic properties, where the binding of a second lower-affinity Mg^{2+} ion is responsible for the decrease in both the apparent Michaelis constant K_{mA}^{app} and the catalytic constant, k_{cat}^{app} (*23*, *34*).

Initially, we predicted that because the Mg^{2+} ion coordination of JNK3 (a MAPK) and cAPK are so similar, the binding of a second magnesium ion would inhibit ERK2, in line with the cAPK kinetics. However, this turned out not to be the

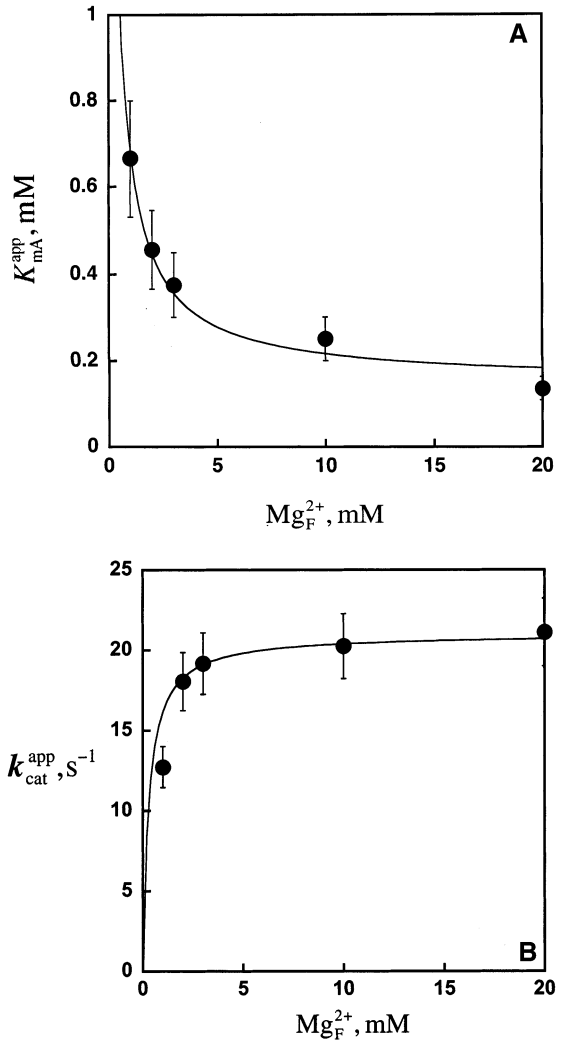

FIGURE 1: (A) Dependence of K_{mA}^{app} on the concentration of free magnesium, Mg_F^{2+}, for the phosphorylation of EtsΔ138 by ERK2 at 27 °C, pH 8.0, and an ionic strength of 0.15 M (KCl). Initial velocities (v) were measured using 2 nM ERK2, 25 mM HEPES, and 2 mM DTT. The concentration of ATP^{4-} was varied from 0.033 to 4 mM at fixed concentrations of free magnesium, Mg_F^{2+} (1, 2, 3, 10, or 20 mM), and EtsΔ138 (150 μM). Values of K_{mA}^{app} were obtained by fitting the observed velocities (v) to eq 6. The line though the data is a nonlinear least-squares fit to eq 11 according to the parameters in Table 2. (B) Dependence of k_{cat}^{app} on the concentration of free magnesium, Mg_F^{2+}, for the phosphorylation of EtsΔ138 by ERK2 at 27 °C, pH 8.0, and an ionic strength of 0.15 M (KCl). Initial velocities (v) were measured using 2 nM ERK2, 25 mM HEPES, and 2 mM DTT. The EtsΔ138 concentration was varied from 4 to 200 μM at various concentrations of Mg_F^{2+} (0.5, 2, 3, 10, and 20 mM) and ATP^{4-} (4 mM). Values of k_{cat}^{app} were obtained by fitting v to eq 6 using nonlinear least-squares fitting methods. The line through the data corresponds to a fit to eq 10 according to the parameters in Table 2.

case. In fact, Figure 1B shows that rather than inhibiting ERK2, an increase in the Mg_F^{2+} concentration (from 1 to 20 mM) leads to a 1.5-fold increase in k_{cat}^{app} (from 13 to 20 s^{-1}). Thus, despite many similarities in both sequence and structure, the kinetic mechanisms of cAPK and ERK2 appear to differ with respect to the role of Mg^{2+} ions. The increase in k_{cat}^{app} raised the possibility that a second magnesium ion is an activator of ERK2. Therefore, because ERK2 is present as the ERK2·EtsΔ138 complex in the experiment described

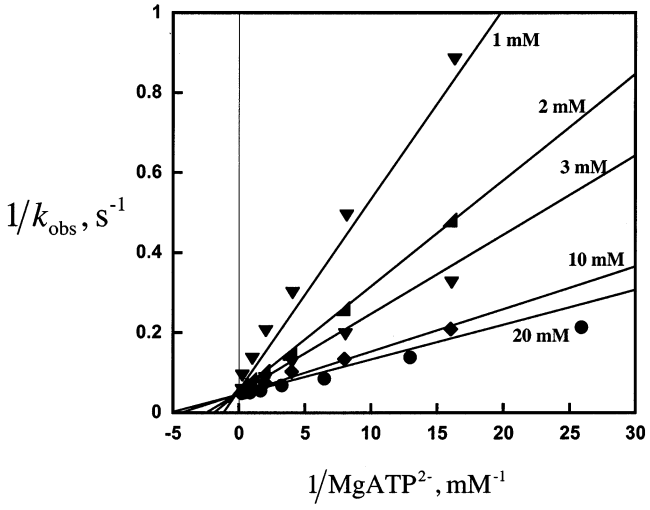

FIGURE 2: Plot of $1/v$ vs $1/[Mg^{2+}ATP^{4-}]$ at fixed concentrations of Mg_F^{2+} (as indicated) and 150 μM EtsΔ138. Initial velocities (v) were measured using 2 nM ERK2, 2 mM DTT 0.034−4.3 mM $Mg^{2+}ATP^{4-}$, and 1−20 mM Mg_F^{2+} at pH 8.0, 27 °C, and an ionic strength of 0.15 M (KCl). The lines through the data are nonlinear least-squares fits to eq 7.

Table 2: Kinetic Parameters for the Phosphorylation of EtsΔ138 by ERK2 According to Scheme 2B[a]

parameter	value[b]	parameter	value[b]
k_{cat}	20.3 ± 0.5 s^{-1}	K_{mA}	94 ± 12 μM
K_0	31 ± 3 μM	K_{iB}	5500 ± 1100 μM
K_{iA}	2200 ± 440 μM[c]	K_{mB}	235 ± 42 μM

[a] Initial velocities were measured using 2 nM ERK2 and 2 mM DTT at pH 8.0, 27 °C, and an ionic strength of 0.15 M (KCl). [b] Derived by global fitting of initial velocities (v) to eq 12. [c] Derived from the relationship $K_{mA}K_{iB} = K_{mB}K_{iA}$.

above, we treated the kinetic data initially as a two-component activator−substrate system, where Mg^{2+} and $MgATP^{2-}$ bind to the enzyme complex, ERK2·EtsΔ138. Such a system resembles, at least conceptually, a ternary complex mechanism and is described by eq 7,[5] for the case where the activator is essential. The plots in panels A and B of Figure 1 which show fits according to eqs 11 and 10, respectively, lend support to the notion that a second magnesium ion activates ERK2.

The kinetic data can also be plotted as a double-reciprocal plot according to eq 7. Such a plot of $1/v$ versus $1/[MgATP^{2-}]$, at a fixed "'saturating" concentration of EtsΔ138 and various concentrations of free magnesium (Mg_F^{2+}), reveals a linear pattern of lines that intersect at a common vertical coordinate above the x-axis (Figure 2).[6] This plot is also consistent with the notion that a magnesium ion activates ERK2. The kinetic parameters describing these fits are presented in Table 2 and were obtained by a global analysis approach, which is described below. The plot of $1/v$ versus $1/[Mg_F^{2+}]$ at various

[5] Equation 7 was derived for a random order ternary complex mechanism with the assumption that all the steps prior to the interconversion of the enzyme-bound substrates to enzyme-bound products are at equilibrium. Within experimental error, eq 7 generally describes the initial rate of a reaction for both a random order and compulsory order ternary complex mechanism.

[6] While this plot is consistent with a rapid equilibrium ordered mechanism, inhibition studies with 5-iodotubericidin, outlined below, suggest that this is not the case.

Scheme 4: Random Ordered Binding Model for the Activation of ERK2 by Mg^{2+}

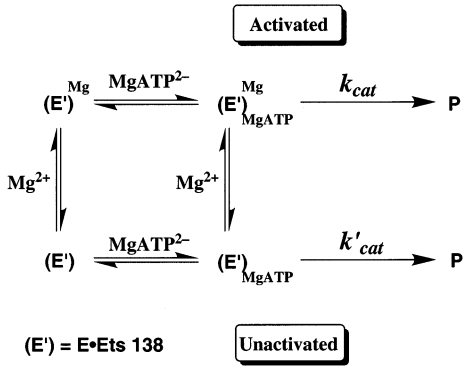

concentrations of $MgATP^{2-}$ at saturating EtsΔ138 (not shown) shows a pattern of intersecting lines that also intersect above the *x*-axis in accordance with the proposed mechanism.

Evidence that Mg^{2+} Is an Essential Activator of ERK2. The above analysis is limited by the imposed experimental constraints, which require a large extrapolation to low concentrations of Mg^{2+} to assess whether the metal ion is *essential*. This is most apparent in Figure 1B where k_{cat}^{app} varies less than 2-fold over the entire range that was studied. To address whether the second Mg^{2+} ion is an essential activator requires a kinetic analysis at low concentrations of Mg_F^{2+}. To do this, we took an approach that has been applied to the study of a number of metal ion-dependent enzymes, which is summarized in a particularly useful review by Morrison (*35*). This approach is to individually vary the concentration of total magnesium ion (Mg_0^{2+}) or total ATP^{4-} (ATP_0^{4-}) while keeping the concentration of the other ligand constant and measuring the velocity of the reaction. One then obtains a series of velocity profiles as a function of the varied substrate at various cosubstrate concentrations. Using this approach, it is possible to examine the dependence of ERK2 over a full range of Mg^{2+} ion concentrations, and sample a much wider range of observed velocities. Several features of these profiles (as well as the data presented above) are consistent with the kinetic model shown in Scheme 4, for the situation when $k_{cat} \geq 10k_{cat}'$.

To take this approach, it is necessary to fix the concentration of EtsΔ138 close to saturation, which in this case is possible because the K_m for EtsΔ138 varies only slightly with Mg_F^{2+} concentration (Table 1). We chose to keep the concentration of EtsΔ138 at 150 μM to prevent protein precipitation and to avoid potential solvent effects caused by high protein concentrations in the solution. While ERK2 is not fully saturated by 150 μM EtsΔ138 under all of the experimental conditions that were employed, the values of K_{mC}^{app} in Table 1 suggest that the degree of saturation by EtsΔ138 varies by less than 5% over the entire range of Mg_F^{2+} concentrations that were employed. This variation is well within the limits of error and unlikely to have a significant impact on kinetic modeling.

We first varied the concentration of total magnesium (Mg_0^{2+}) at different fixed levels of ATP_0^{4-} to obtain velocity profiles, several of which are shown in panels A and B of Figure 3. According to the mechanism in Scheme 4, when $k_{cat} \geq k_{cat}'$, the velocity profiles reflect the competition

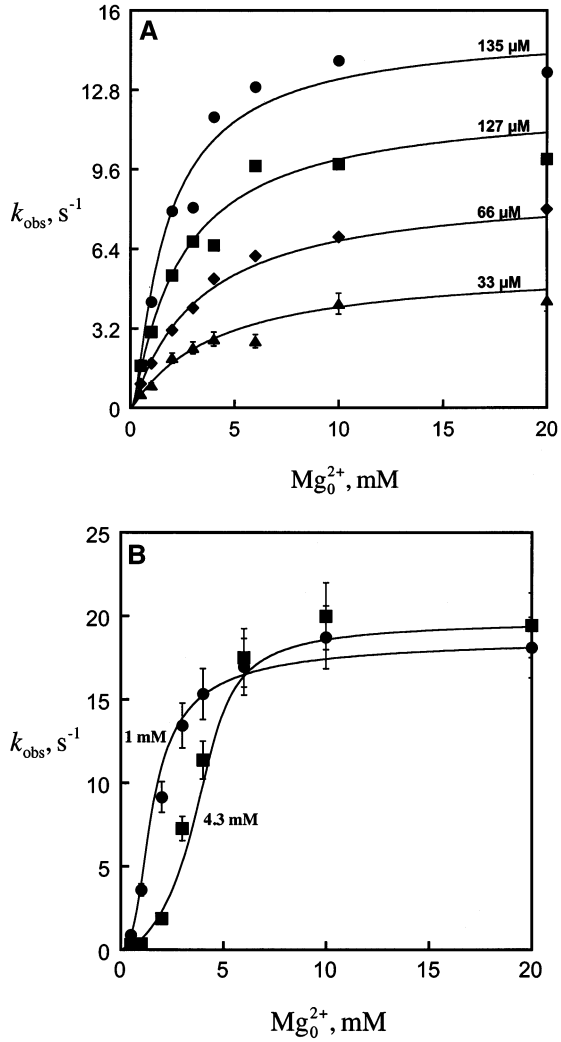

FIGURE 3: (A) Magnesium velocity profiles at low concentrations of total ATP^{4-} (ATP_0^{4-}) for the phosphorylation of EtsΔ138 by ERK2 at 27 °C, pH 8.0, and an ionic strength of 0.15 M (KCl). Initial velocities were measured using 2 nM ERK2, 25 mM HEPES, and 2 mM DTT at varied concentrations of Mg_F^{2+} (0−5 mM) and various concentrations of ATP^{4-} (33, 66, 127, and 135 μM). The solid lines represent the best global fit to eq 12 according to the parameters in Table 2. (B) Magnesium velocity profiles at high concentrations of total ATP^{4-} (ATP_0^{4-}) for the phosphorylation of EtsΔ138 by ERK2 at 27 °C, pH 8.0, and an ionic strength of 0.1 M (KCl). Initial velocities were measured using 2 nM ERK2, 25 mM HEPES, and 2 mM DTT at varied concentrations of Mg_0^{2+} (0−5 mM) and fixed varied concentrations of ATP^{4-} (1 and 4.3 mM). The solid lines represent the best global fit to eq 12 according to the parameters in Table 2.

between the enzyme complexes (E′) and $(E')_{MgATP}$ and the nucleotide, ATP^{4-}, for the unbound magnesium that is free in solution. Thus, at high levels of ATP_0^{4-} (≥1 mM), a sigmoidal curve is clearly apparent (Figure 3B). According to Scheme 4, this follows because when the ATP_0^{4-} concentration is in excess of total magnesium (Mg_0^{2+}) the free magnesium (Mg_F^{2+}) is sequestered in the form of $MgATP^{2-}$, which has a dissociation constant of 31 μM. Under these conditions, little free Mg^{2+} is available to bind the enzyme complexes, and therefore, the concentration of the activated form of the enzyme, $(E')_{MgATP}^{Mg}$, remains low. As the concentration of Mg_0^{2+} approaches that of ATP_0^{4-}, Mg_F^{2+} becomes increasingly more available to the

enzyme and the concentration of $(E')^{Mg}_{MgATP}$, and hence the observed velocity (v), increases rapidly. At low concentrations of ATP_0^{4-} (30−540 μM), the velocity profiles in Figure 3A are concave throughout, because ATP_0^{4-} does not effectively sequester Mg_F^{2+} at these concentrations, and therefore, a simple hyperbolic binding dependence on Mg_0^{2+} concentration is observed. Scheme 4 also explains why the ascending limb of the velocity profiles in Figure 3B is shifted downward as the fixed concentration of AT P_0^{4-} is increased. In this case, the high concentration of AT P_0^{4-} results in a relatively lower concentration of Mg_F^{2+} and consequently less "activated" $(E')^{Mg}_{MgATP}$. At high concentrations of Mg_0^{2+} (20 mM, Figure 3B), the enzyme is fully active as predicted by Scheme 4. The absence of inhibition shows that Mg^{2+} does not trap the enzyme in an inactive form or bind to a low-affinity site that partially inhibits the enzyme.

We also varied the ATP_0^{4-} concentration at different fixed concentrations of Mg_0^{2+}. Several of the velocity profiles obtained are shown in panels A and B of Figure 4. All these profiles are concave and shifted upward at higher concentrations of magnesium as predicted by population of the $(E')^{Mg}_{MgATP}$ species in Scheme 4. At lower concentrations of Mg_0^{2+}, a peak in the velocity profile is seen, which is consistent with titration of the enzyme from the activated $(E')^{Mg}_{MgATP}$ complex to the unactivated $(E')_{MgATP}$ complex (Figure 4A). It should be recalled that when the concentration of ATP_0^{4-} approaches that of Mg_0^{2+} most, but not all, is sequestered in the form of the $MgATP^{2-}$ complex. As the concentration of ATP_0^{4-} is increased further, the availability of Mg_F^{2+} decreases considerably and the velocity approaches a low limiting value as the proportion of the unactivated enzyme increases.

All the kinetic data were fitted to eq 12 that describes the mechanism of Scheme 4, when $k_{cat} > k_{cat}'$.[7] It should be noted that the equilibrium in Scheme 3 is included in the global fitting process. Final parameters are presented in Table 2. In general, the agreement between the observed and calculated velocities in Figures 3 and 4 is excellent (to within 20%), apart from several values obtained at very low concentrations of Mg_F^{2+}, where the sensitivity to the concentration of Mg_F^{2+} is high. We also tested the possibility that Mg^{2+} is a nonessential activator of ERK2 where the unactivated complex $(E')_{MgATP}$ in Scheme 4 has a significant level of activity; i.e., $k_{cat} \sim k_{cat}'$. Equation 13, derived by assuming the enzyme species are in rapid equilibrium, was used to assess this model. If the unactivated species, $(E')_{MgATP}$, does have significant activity, it will be most apparent under conditions where the enzyme is not activated, i.e., where the fraction of $(E')^{Mg}_{MgATP}$ is low, such as at high concentrations of ATP^{4-}, where all the free magnesium is sequestered in the form of $MgATP^{2-}$. In Figure 4A, the observed velocity is less than 10% of the observed maximal velocity and tends toward zero as the concentration of ATP^{4-} and the fraction of the unactivated enzyme increase. Thus, the velocity profile does not support a model where $(E')_{MgATP}$ has significant activity. While a global fitting analysis of the data using eq 13 predicts that k_{cat}' is essentially zero, a small level of activity ($k_{cat}' \sim 0.1k_{cat}$) that is within the error of the fitting cannot be ruled out.

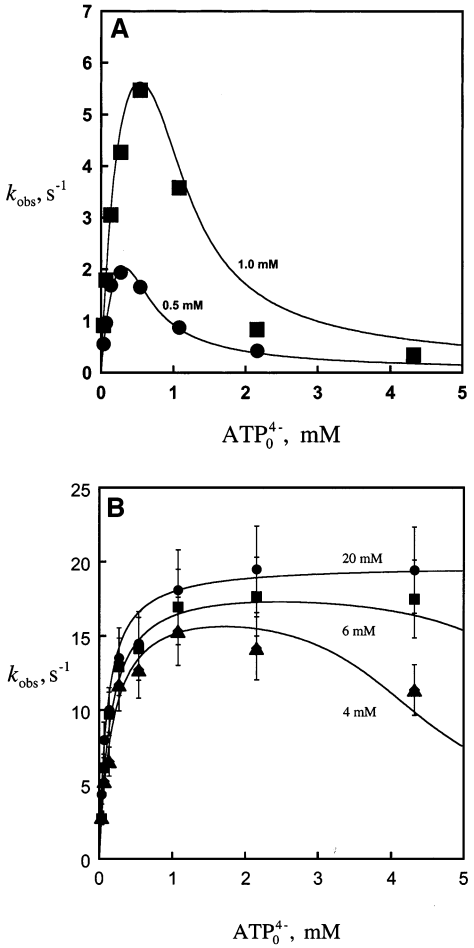

FIGURE 4: (A) ATP velocity profiles at low concentrations of total magnesium, Mg_0^{2+}, for the phosphorylation of EtsΔ138 by ERK2 at 27 °C, pH 8.0, and an ionic strength of 0.15 M (KCl). Initial velocities were measured using 2 nM ERK2, 25 mM HEPES, and 2 mM DTT at varied concentrations of ATP^{4-} (0−20 mM) and various concentrations of total magnesium (0.5 and 1.0 mM). The solid line represents the best global fit to eq 12 according to the parameters in Table 2. (B) ATP velocity profiles at high concentrations of total magnesium, Mg_0^{2+}, for the phosphorylation of EtsΔ138 by ERK2 at 27 °C, pH 8.0, and an ionic strength of 0.15 M (KCl). Initial velocities were measured using 2 nM ERK2, 25 mM HEPES, and 2 mM DTT at varied concentrations of ATP^{4-} (0−20 mM) and various concentrations of total magnesium (4, 6, and 20 mM). The solid line represents the best global fit to eq 12 according to the parameters in Table 2.

Evidence that ATP^{4-} and $KATP^{3-}$ Do Not Inhibit ERK2. The conclusions presented above are based on the assumption that ATP^{4-} does not inhibit ERK2. To test the possibility that ERK2 is inhibited by ATP^{4-} or the potassium complex ($KATP^{3-}$), we examined whether ATP^{4-} binds ERK2 under the conditions of the kinetic assay using isothermal titration calorimetry. The dissociation constant [$K_0' = 66$ mM (Scheme 3)] indicates that under the conditions of the kinetic assay ATP^{4-} and $KATP^{3-}$ are present in similar amounts. Significantly, under the buffer conditions of the assay, no heat change was detected upon addition of up to 2 mM ATP^{4-} to a 65 μM solution of ERK2 (Figure 5A). In contrast, when ERK2 (12.5 μM) was titrated with 5-iodotubericidin (5-IT), a nucleotide analogue, to a molar ratio of 2.5, a significant change in the heat of solution was detected, which

[7] Equation 12 is of the same mathematical form as eq 7.

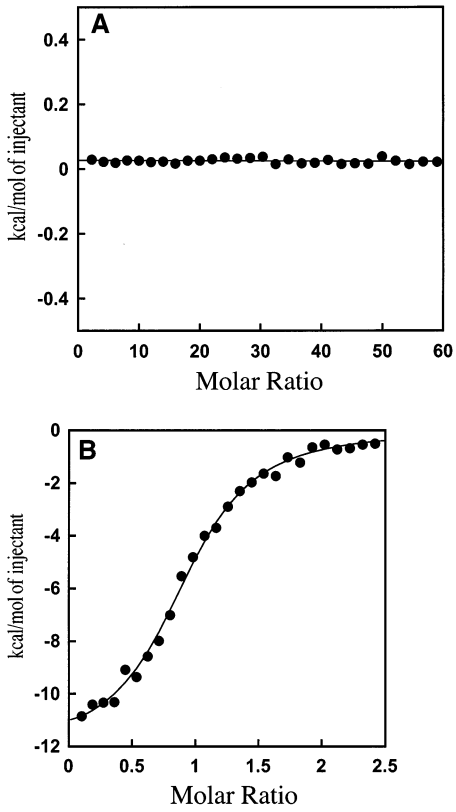

FIGURE 5: (A) Isothermal titration calorimetric analysis of ATP^{4-} binding to ERK2. Plot of the heat generated vs the molar ratio of ligand to protein (ATP^{4-}/ERK2). (B) Isothermal titration calorimetric analysis of 5-IT binding to ERK2. Plot of the heat generated vs the molar ratio of ligand to protein (5-IT/ERK2).

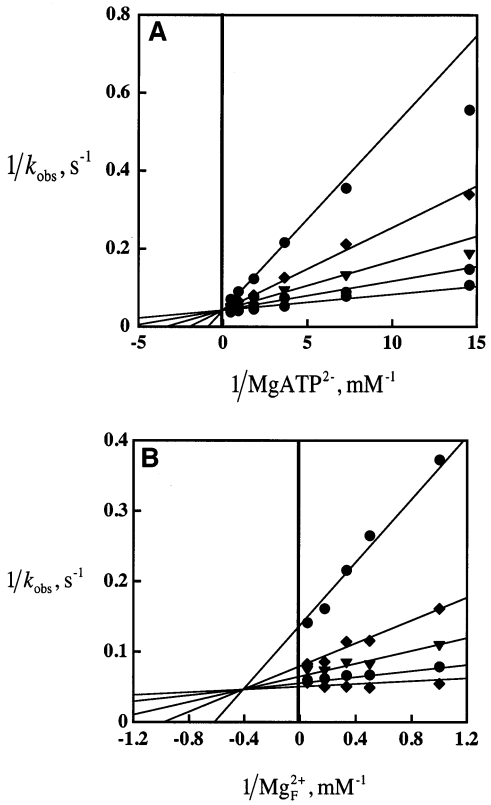

FIGURE 6: (A) Plot of $1/v$ vs $[MgATP^{2-}]$ (0.069−2.2 mM) at various concentrations of 5-iodotubercidin (0−5 μM) and EtsΔ138 (150 μM). Initial velocities were measured using 2 nM ERK2, 20 mM Mg_F^{2+}, and 2 mM DTT at pH 8.0, 27 °C, and an ionic strength of 0.15 M (KCl). The lines through the data correspond to the best fit to the data according to eq 8. (B) Plot of $1/v$ vs $[Mg_F^{2+}]$ (1.0−19 mM) at various concentrations of 5-iodotubercidin (0−10 μM) and EtsΔ138 (150 μM). Initial velocities were measured using 2 nM ERK2, 1 mM $MgATP^{2-}$, and 2 mM DTT at pH 8.0, 27 °C, and an ionic strength of 0.15 M (KCl). The lines through the data correspond to the best fit to the data according to eq 9.

is consistent with the known ability of 5-IT to inhibit the enzyme (Figure 5B). By integrating the experimental isotherm using a single-site binding model, we obtained a binding stoichiometry n of 0.947 ± 0.013 with a dissociation constant K_d of 1.050 ± 0.091 μM, characterized by the following thermodynamic parameters: $\Delta G = -12.1 \pm 0.24$ kcal/mol, $\Delta H = -8.2$ kcal/mol, and $\Delta S = 0.013$ kcal mol^{-1} K^{-1}. The results suggest that 2 mM ATP^{4-} does not significantly bind ERK2 in the presence of KCl ($I = 0.15$). This inability to bind ATP^{4-} is in accord with cAPK, which also binds ATP^{4-} weakly in the absence of Mg^{2+} (*36*). This suggests that charge neutralization by Mg^{2+} is important for the binding of ATP^{2-} to ERK2 and lends support to the kinetic model in Scheme 4. In particular, it rules out inhibition by ATP^{4-} as the reason for the decrease in velocity at high concentrations of ATP^{4-} in Figure 4A.

Probing the Order of Ligand Binding Using Inhibitors. The data presented above provide evidence that Mg^{2+} is an essential activator of ERK2. Interestingly, the point at which the lines intersect in Figure 2 is close (within error) to the ordinate axis and is therefore consistent with a rapid equilibrium ordered mechanism where Mg^{2+} binds to the ERK2·EtsΔ138 complex before $MgATP^{2-}$. However, such a mechanism would be unusual given the number of known structures of protein kinases complexed to just $MgATP^{2-}$ or an analogue. An alternative and more likely explanation for the proximity of the point of intersection to the ordinate axis is that $MgATP^{2-}$ and Mg^{2+} interact favorably upon binding to the ERK2·EtsΔ138 complex. To rule out the ordered mechanism, we examined the mode of ERK2 inhibition by 5-iodotubericidin (5-IT). On the basis of its molecular structure, 5-IT is expected to compete with $MgATP^{2-}$ for ERK2. Figure 6A shows a plot of $1/v$ versus $1/[MgATP^{2-}]$ at various concentrations of 5-IT and saturating Mg^{2+} (20 mM). The best fit to the data according to eq 8 and the parameters in Table 3 clearly shows that, as expected, 5-IT is a competitive inhibitor toward $MgATP^{2-}$. The intercept on the ordinate suggests that no inhibition occurs at saturating $MgATP^{2-}$ concentrations and is consistent with the notion that 5-IT and $MgATP^{2-}$ cannot bind to the same form of the enzyme at the same time.

Figure 6B shows a plot of $1/v$ versus $1/[Mg_F^{2+}]$ at various concentrations of 5-IT and saturating $MgATP^{2-}$ (1 mM). The best fit to the data according to eq 9 and the parameters in Table 3 shows that 5-IT is a mixed inhibitor toward Mg^{2+}. In this case, extrapolation to saturating Mg^{2+} does not result in the absence of inhibition as the lines do not intercept on the axis. Such an inhibition pattern is consistent with the notion that 5-IT binds both the free form of ERK2 and a form of the enzyme that can bind Mg^{2+}. While it is plausible that 5-IT facilitates Mg^{2+} binding, the simplest explanation is that a kinetically significant magnesium binding site is present on the free enzyme. Figure 6B does not support an ordered binding mechanism where Mg^{2+} must bind before $MgATP^{2-}$. For such a mechanism, a parallel set of lines is

Table 3: 5-Iodotubericidin Inhibition Patterns for the Phosphorylation of EtsΔ138 by ERK2[a]

varied substrate	fixed substrate	fixed saturating substrate	mechanism	k_{cat} (s^{-1})	K_{iC}^{app} (μM)	K_{iU}^{app} (μM)
$MgATP^{2-}$ [b]	Mg^{2+} [c]	EtsΔ138[h]	mixed[g]	20	0.494 ± 0.042	6.37 ± 0.71
Mg^{2+} [d]	$MgATP^{2-}$ [e]	EtsΔ138[h]	competitive[f]	24	0.473 ± 0.058	

[a] Initial velocities were measured using 2 nM ERK2, 2 mM DTT, EtsΔ138 (150 μM), and 5-IT (0−5 μM) at pH 8.0, 27 °C, and an ionic strength of 0.15 M (KCl). [b] At 0.069 to 2200 μM. [c] At 20 mM. [d] At 1−19 mM. [e] At 1 mM. [f] Best fit of the data according to eq 8 for competitive inhibition. [g] Best fit of the data according to eq 9 for mixed inhibition. [h] At 150 μM.

expected, not the mixed inhibition pattern that is observed in Figure 6B. Thus, we conclude that $MgATP^{2-}$ can bind the free enzyme and is not dependent on the prior binding of Mg^{2+}.

To test whether $MgATP^{2-}$ must bind ERK2 before Mg^{2+}, several divalent metal ions were tested as potential competitive inhibitors for the second Mg^{2+} ion. The goal was to try to find a metal ion that competes cleanly with the second Mg^{2+} ion without disrupting the $MgATP^{2-}$ complex. Potentially, this could then be used in a manner analogous to that of 5-IT. Unfortunately, none of the inhibitory metals that were tested (Be^{2+}, Co^{2+}, and Zn^{2+}) were found to be useful inhibitors, as they were found to compete with Mg^{2+} for the binding to ATP^{4-}. No inhibition by Ni^{2+} and Cd^{2+} was detected, while Mn^{2+} supported catalysis.

We propose that ERK2 follows the random ordered binding mechanism shown in Scheme 4 or an ordered mechanism where $MgATP^{2-}$ binds before Mg^{2+} (bottom pathway). In either case, Mg^{2+} is proposed to be an essential activator where $k_{cat} > 10k_{cat}'$.

Phosphoryl Transfer and Magnesium Ions. By virtue of its physical properties, magnesium is the only divalent cation, present *in vivo* at concentrations of >1 μM, that has a strong affinity for polyphosphate ions. Consequently, ATP^{4-} is complexed exclusively to Mg^{2+} in cells (*37*). It is reasonable to assume therefore that protein kinases have evolved to utilize the Mg^{2+} complex of ATP^{4-} as a substrate, rather than the free ATP^{4-} ion. While it is certainly plausible that magnesium has a catalytic role, it is interesting that magnesium ions provide little rate enhancement for the hydrolysis of ATP^{4-} (*38*). It is therefore particularly interesting that ERK2 appears to require the binding of two magnesium ions to achieve physiologically relevant catalysis. In solution, phosphoryl transfer from ATP^{4-} to a hydroxyl nucleophile is characterized by a dissociative transition state with little O−P bond formation between the nucleophile and the terminal phosphate and extensive cleavage of the bond between the bridging oxygen of the departing ADP^{3-} and the phosphorus of the γ-phosphoryl moiety (*38*). The current view is that a similar mechanism prevails at the active site of a protein kinase (*39*), although this view is not universally accepted (*40*). For such a mechanism, the majority of charge buildup is expected to be located on the leaving group oxygen, with little (if any) on the γ-phosphoryl moiety (*38*). While the judicial placement of a magnesium ion conceivably stabilizes this charge buildup and promotes catalysis, it is not clear what kinetic advantage two metal ions provide.

In addition, the mechanism of ERK2 is intriguing, because it differs from that of cAPK and other serine/threonine protein kinases that bind two magnesium ions. The kinetic investigation of Shaffer and Adams suggests that, while the magnesium ion at the high-affinity M2 site (Scheme 2A) plays a significant role in promoting phosphoryl transfer, the corresponding magnesium ion at the low-affinity M1 site (Scheme 2A) does not (*22*, *23*). Given that both metal ions coordinate ATP^{4-} in a similar manner in the structure of cAPK complexed with a transition state mimic (*24*), the apparent differences are surprising.

Within the protein kinase family, a common chemical mechanism is expected on the basis of the conservation of a number of key catalytic residues (*41*). Why then, given the predicted similarity in magnesium coordination between ERK2 and cAPK, does cAPK require only one bound magnesium ion for efficient phosphoryl transfer whereas ERK2 requires two?[8] Studies on cAPK (*42*) suggest that conformational changes are an integral part of the catalytic cycle of this enzyme. In fact, two potential conformational transitions were identified in cAPK, whose rates are sensitive to the presence of the low-affinity M1 magnesium (*22*, *23*). One conformational step occurs before phosphoryl transfer, while the second occurs after. It is plausible that magnesium-sensitive conformational effects could be the source of the differences between cAPK and ERK2. Alternatively, it is possible that ERK2 binds Mg^{2+} in a manner different from that of cAPK. While the structure of the related MAPK, JNK3, does not support this latter hypothesis, X-ray crystallography can be misleading in cases where nonfunctional complexes or substrate analogues are employed. Thus, it is possible (as pointed out by a referee) that some of the reported structures, including the JNK3 binary complex, reflect an experimental artifact. Taken together, however, the available evidence suggests that subtle differences, perhaps in the conformational energetics of the protein kinases in the presence and absence of bound magnesium ions, offer the most reasonable explanation for the different requirements for magnesium between cAPK and ERK2.

In Table 4, we have summarized the kinetic data of several other protein kinases whose steady state parameters have been determined over a range of metal ion concentrations. It is clear from this table that these protein kinases display a wide variation in their dependency on metal ion concentration. Of note are the protein tyrosine kinases, the insulin receptor, VEGF, Csk, and cSRC. Like ERK2, all four appear to be activated by divalent metal ions, and in the case of Csk, direct evidence for the importance of γ-phosphoryl metal ion interactions in the reaction mechanism is well-established (*43*). Interestingly, however, the coordination of the metal ions in the insulin receptor differs significantly from that of cAPK (Scheme 2B). It will be interesting to see if this is the case for the other tyrosine kinases also.

[8] Under pre-steady state conditions, the phosphorylation of EtsΔ138 by ERK2 displays a "burst" with an amplitude of less than unity. This corresponds to partially rate-limiting phosphorylation of EtsΔ138 and product release (W. F. Waas, M. Rainey, and K. N. Dalby, manuscript in preparation).

Table 4: Metal Ion Dependence of the Steady State Parameters for a Number of Protein Kinases[a]

type	specificity	protein kinase	substrate	V_{max}^{app}	K_{mA}^{app}	K_{mC}^{app}
nonreceptor	Ser/Thr	cAPK[b]	LRRAS*LG	↓	↓	no change
receptor	Tyr	*v*-FPS[c]	EAEIY*EAIE	no change	↓	no change
receptor	Tyr	FGFR[d]	poly-E_4Y	↑	↓	↑
		insulin receptor[e]				
		VEGFR[f]				
nonreceptor	Ser/Thr	ERK2[g]	Ets138	↑	↓	↑
nonreceptor	Tyr	Csk[d,h]	poly-E_4Y	↑	no change	↑
		SRC[d]				

[a] Steady state parameters are transparent to the individual kinetic steps that contribute to the observed steady state velocity. The arrows indicate whether the apparent steady state parameter increased (↑), decreased (↓), or was unaffected with increasing concentrations of uncomplexed divalent metal ion. [b] The decrease in V_{max}^{app} as the concentration of free magnesium increases is thought to be due to a decrease in the rate of product release ($k \sim 25\ s^{-1}$) and not phosphoryl transfer, which is fast ($k > 500\ s^{-1}$) (*47*). [c] Free magnesium is reported to affect the dissociation constant of $Mg^{2+}ATP^{4-}$ (*33*). Phosphoryl transfer ($k \sim 40-100\ s^{-1}$) and product release ($k \sim 17-22\ s^{-1}$) are reported to be partially rate-limiting (*48*). The effect of free magnesium on these steps has not been reported. [d] It has not been established whether two metal ions are *essential* for catalytic activity (*45*). [e] Observed with Mn^{2+}, but not with Mg^{2+} (*49*). The coordination of metal ions at the active site of the insulin receptor appears to be distinct from that of the serine/threonine specific protein kinases (*50*). [f] Exhibits a velocity dependence on substrate and product concentrations that is consistent with a random ordered reactant kinetic mechanism (*46*). [g] This work. Two magnesium ions are essential for high catalytic activity. [h] Using $K_4E_2IYF_3$ as the substrate, phosphoryl transfer was reported to be fast and reversible ($k_f \geq 140\ s^{-1}$, $k_b = 25\ s^{-1}$) with product release ($k = 0.6\ s^{-1}$) being rate-limiting (*51*).

Physiological Concentrations of Mg^{2+}: Possible Implications. It is notable that the physiological concentrations of Mg_F^{2+} and $MgATP^{2-}$ lie close to 0.5 and 5−15 mM, respectively, because the kinetic modeling suggests that under these conditions activated ERK2 is between 59 and 65% active. The significance of this is difficult to discern, however, because it is not currently clear how total magnesium, Mg_0^{2+}, is distributed between cytosolic organelles, or how its concentration varies throughout the cell cycle. There is some evidence that resting and proliferating cells may differ with respect to their magnesium content and compartmentalization, although the changes may be small (*44*). Thus, while there is potential for ERK2 to be regulated through changes in the level of Mg_F^{2+}, there is currently no evidence to support such a mechanism *in vivo*. As divalent magnesium is the only divalent cation present in cells at a concentration in excess of 1 μM (*37*), it appears unlikely that other cations will play a role in regulating the enzyme. However, it is plausible that the affinity of ERK2 for magnesium ions is regulated *in vivo* by small molecules or other proteins. Interestingly, it might be possible to design potentially useful inhibitors of ERK2 that modulate the magnesium binding and hence the activation state of ERK2 rather than directly competing with $MgATP^{2-}$.

CONCLUSION

The data presented here address the composition of the catalytically active ERK2 species and suggest that a second Mg^{2+} ion activates ERK2. While several kinetic studies suggest that a number of tyrosine specific protein kinases, such as Csk (*45*) and VEGFR2 TK (*46*), are likely to exhibit a similar kinetic mechanism, this mechanism has not been demonstrated previously for a serine/threonine specific protein kinase.

ACKNOWLEDGMENT

We are indebted to Dr. Melanie Cobb, Dr. Natalie Ahn, and Dr. Lawrence McIntosh for generously providing us with DNA encoding His_6-ERK2, His_6-MEK1G7B, and His_6-Ets-1^{1-138}, respectively.

REFERENCES

1. Adams, J. A. (2001) *Chem. Rev. 101*, 2271−2290.
2. Niefind, K., Guerra, B., Pinna, L. A., Issinger, O. G., and Schomburg, D. (1998) *EMBO J. 17*, 2451−2462.
3. Niefind, K., Putter, M., Guerra, B., Issinger, O. G., and Schomburg, D. (1999) *Nat. Struct. Biol. 6*, 1100−1103.
4. Niefind, K., Guerra, B., Ermakowa, I., and Issinger, O. G. (2001) *EMBO J. 20*, 5320−5331.
5. Ryazanov, A. G., Ward, M. D., Mendola, C. E., Pavur, K. S., Dorovkov, M. V., Wiedmann, M., Erdjument-Bromage, H., Tempst, P., Parmer, T. G., Prostko, C. R., Germino, F. J., and Hait, W. N. (1997) *Proc. Natl. Acad. Sci. U.S.A. 94*, 4884−4889.
6. Steinbacher, S., Hof, P., Eichinger, L., Schleicher, M., Gettemans, J., Vandekerckhove, J., Huber, R., and Benz, J. (1999) *EMBO J. 18*, 2923−2929.
7. Yamaguchi, H., Matsushita, M., Nairn, A. C., and Kuriyan, J. (2001) *Mol. Cell 7*, 1047−1057.
8. Fieulaine, S., Morera, S., Poncet, S., Monedero, V., Gueguen-Chaignon, V., Galinier, A., Janin, J., Deutscher, J., and Nessler, S. (2001) *EMBO J. 20*, 3917−3927.
9. Taylor, S. S., Buechler, J. A., Slice, L. W., Knighton, D. K., Durgerian, S., Ringheim, G. E., Neitzel, J. J., Yonemoto, W. M., Sowadski, J. M., and Dospmann, W. (1988) *Cold Spring Harbor Symp. Quant. Biol. 53* (Part 1), 121−130.
10. Pearson, G., Robinson, F., Beers Gibson, T., Xu, B. E., Karandikar, M., Berman, K., and Cobb, M. H. (2001) *Endocr. Rev. 22*, 153−183.
11. Hoshino, R., Chatani, Y., Yamori, T., Tsuruo, T., Oka, H., Yoshida, O., Shimada, Y., Ari-i, S., Wada, H., Fujimoto, J., and Kohno, M. (1999) *Oncogene 18*, 813−822.
12. Sebolt-Leopold, J. S., Dudley, D. T., Herrera, R., Van Becelaere, K., Wiland, A., Gowan, R. C., Tecle, H., Barrett, S. D., Bridges, A., Przybranowski, S., Leopold, W. R., and Saltiel, A. R. (1999) *Nat. Med. 5*, 810−816.
13. Sharrocks, A. D., Yang, S. H., and Galanis, A. (2000) *Trends Biochem. Sci. 25*, 448−453.
14. Waas, W. F., and Dalby, K. N. (2001) *Protein Expression Purif. 23*, 191−197.
15. Waas, W. F., and Dalby, K. N. (2002) *J. Biol. Chem. 277*, 12532−12540.
16. Yang, B. S., Hauser, C. A., Henkel, G., Colman, M. S., Van Beveren, C., Stacey, K. J., Hume, D. A., Maki, R. A., and Ostrowski, M. C. (1996) *Mol. Cell. Biol. 16*, 538−547.
17. Seidel, J. J., and Graves, B. J. (2002) *Genes Dev. 16*, 127−137.
18. Armstrong, R. N., Kondo, H., Granot, J., Kaiser, E. T., and Mildvan, A. S. (1979) *Biochemistry 18*, 1230−1238.
19. Zheng, J., Trafny, E. A., Knighton, D. R., Nguyen, H. X., Taylor, S. S., Ten, E., Lynn, F., and Sowadski, J. M. (1993) *Acta Crystallogr. D49*, 362−365.

20. Lowe, E. D., Noble, M. E., Skamnaki, V. T., Oikonomakos, N. G., Owen, D. J., and Johnson, L. N. (1997) *EMBO J. 16*, 6646−6658.
21. Xie, X., Gu, Y., Fox, T., Coll, J. T., Fleming, M. A., Markland, W., Caron, P. R., Wilson, K. P., and Su, M. S. (1998) *Structure 6*, 983−991.
22. Shaffer, J., and Adams, J. A. (1999) *Biochemistry 38*, 5572−5581.
23. Shaffer, J., and Adams, J. A. (1999) *Biochemistry 38*, 12072−12079.
24. Madhusudan, Akamine, P., Xuong, N. H., and Taylor, S. S. (2002) *Nat. Struct. Biol. 9*, 273−277.
25. Adams, J. A., and Taylor, S. S. (1993) *Protein Sci. 2*, 2177−2186.
26. Zhang, F., Robbins, D. J., Cobb, M. H., and Goldsmith, E. J. (1993) *J. Mol. Biol. 233*, 550−552.
27. Slupsky, C. M., Gentile, L. N., Donaldson, L. W., Mackereth, C. D., Seidel, J. J., Graves, B. J., and McIntosh, L. P. (1998) *Proc. Natl. Acad. Sci. U.S.A. 95*, 12129−12134.
28. Gill, S. C., and von Hippel, P. H. (1989) *Anal. Biochem. 182*, 319−326.
29. O'Sullivan, W. J., and Perrin, D. D. (1964) *Biochemistry 3*, 18−26.
30. Watanabe, S., Trosper, T., Lynn, M., and Evenson, L. (1963) *J. Biochem. 54*, 17−26.
31. Watanabe, S., Frantz, W., and Trottier, D. (1963) *Anal. Biochem. 5*, 345−359.
32. Cornish-Bowden, A. (1995) *Fundamentals of Enzyme Kinetics*, 2nd ed., Portland Press, Colchester, U.K.
33. Saylor, P., Wang, C., Hirai, T. J., and Adams, J. A. (1998) *Biochemistry 37*, 12624−12630.
34. Cook, P. F., Neville, M. E., Jr., Vrana, K. E., Hartl, F. T., and Roskoski, R., Jr. (1982) *Biochemistry 21*, 5794−5799.
35. Morrison, J. F. (1979) *Methods Enzymol. 63*, 257−294.
36. Herberg, F. W., Doyle, M. L., Cox, S., and Taylor, S. S. (1999) *Biochemistry 38*, 6352−6360.
37. Fraústo, J. J. R., and Williams, R. J. P. (2001) *The biological chemistry of the elements*, Oxford University Press, Oxford, U.K.
38. Admiraal, S. J., and Herschlag, D. (1995) *Chem. Biol. 2*, 729−739.
39. Kim, K., and Cole, P. A. (1997) *J. Am. Chem. Soc. 119*, 11096−11097.
40. Williams, N. H. (2000) *J. Am. Chem. Soc. 122*, 12023−12024.
41. Taylor, S. S., and Radzio-Andzelm, E. (1994) *Structure 2*, 345−355.
42. Li, F., Gangal, M., Juliano, C., Gorfain, E., Taylor, S. S., and Johnson, D. A. (2002) *J. Mol. Biol. 315*, 459−469.
43. Grace, M. R., Walsh, C. T., and Cole, P. A. (1997) *Biochemistry 36*, 1874−1881.
44. Rubin, A. H., Terasaki, M., and Sanui, H. (1979) *Proc. Natl. Acad. Sci. U.S.A. 76*, 3917−3921.
45. Sun, G., and Budde, R. J. (1997) *Biochemistry 36*, 2139−2146.
46. Parast, C. V., Mroczkowski, B., Pinko, C., Misialek, S., Khambatta, G., and Appelt, K. (1998) *Biochemistry 37*, 16788−16801.
47. Grant, B. D., and Adams, J. A. (1996) *Biochemistry 35*, 2022−2029.
48. Wang, C., Lee, T. R., Lawrence, D. S., and Adams, J. A. (1996) *Biochemistry 35*, 1533−1539.
49. White, M. F., Haring, H. U., Kasuga, M., and Kahn, C. R. (1984) *J. Biol. Chem. 259*, 255−264.
50. Hubbard, S. R. (1997) *EMBO J. 16*, 5572−5581.
51. Shaffer, J., Sun, G., and Adams, J. A. (2001) *Biochemistry 40*, 11149−11155.

BI027171W